JOURNAL OF OPTOELECTRONICS AND ADVANCED MATERIALS Vol. 12, No. 10, October 2010, p. 2139 - 2143

Temperature and frequency dependent dielectric properties of $Au/Bi_4Ti_3O_{12}/SiO_2/Si$ (MFIS) structures

Ş. ALTINDAL, F. PARLAKTÜRK, A. TATAROĞLU*, M.M. BÜLBÜL
Physics Department, Faculty of Arts and Sciences, Gazi University, 06500, Ankara, Turkey

The frequency and temperature dependence of dielectric constant (ε'), dielectric loss (ε''), dielectric loss tangent (tanδ) and the ac electrical conductivity (σ_{ac}) of $Au/Bi_4Ti_3O_{12}/SiO_2/Si$ (MFIS) structures were studied in the frequency range of 1 kHz–5 MHz and in the temperature range of 80-400 K. The dielectric parameters of MFIS structure were calculated from C-V and G/ω-V measurements. It was found that both dielectric and conductivity were quite sensitive to temperature and frequency at relatively high temperatures and at low frequencies. Experimental results show that the ε' and ε'' decrease with increasing frequency, while they increase with increasing temperature. On the other hand, the ac electrical conductivity (σ_{ac}) increases with increasing frequency and temperature alike. The interfacial polarization can be more easily occurred at low frequencies, and the number of interface states density between semiconductor/insulator interfaces, consequently, contributes to the improvement of dielectric properties of MFIS structure. The values of activation energy (E_a) were obtained from the slope of the Ln□ vs q/kT plots, and found as 122.3 meV and 109.3 meV for 100 kHz and 500 kHz, respectively. In addition, the real *(M')* and imaginary *(M'')* components of the electrical modulus were calculated from the values of ε' and ε'' for two different frequencies. It was found that the values of real component M' decreases with increasing temperature up to room temperature, and then becomes independent of temperature and frequency.

(Received September 8, 2010; accepted October 14, 2010)

Keywords: Au-/n-Si(111) SBDs, I-V-T and C-V-T caharacteristics, Interface states, Series resistance, Norde function

1. Introduction

$Bi_4Ti_3O_{12}$ (BTO) is a typical ferroelectric material with useful properties for devices such as non-volatile ferroelectric random access memories (FRAMs), optical memory, piezoelectric, and electro-optic devices [1-4]. Ferroelectric (BTO) thin films that sandwiched in metal electrodes have been extensively studied and developed as FeRAMs [5].

In order to realize FeRAMs, a metal-ferroelectric-metal (MFM) type capacitor has been widely investigated [6-8]. Another ferroelectric memory is the ferroelectric field effect transistor (Fe, FET), which uses ferroelectric thin films as the gate oxide in a field effect transistor (FET) to form a metal-ferroelectric-semiconductor (MFS) structure.

In such structure, the surface potential of the semiconductor is controlled by the remnant polarization of the ferroelectric thin films. Using a thin interfacial insulator layer such as SiO_2, Si_xN_y, CeO_2 and Al_2O_3 at the BTO/Si interface, MFS structure is converted to MFIS structure. This interfacial insulator layer cannot only prevent inter-diffusion between ferroelectric film (BTO) and silicon (Si) substrate, but also alleviate the electric field reduction issue in MFIS structure [9,10]. Recently, the devices such as metal-ferroelectric-metal (MFM), metal-ferroelectric-semiconductor (MFS) and metal-ferroelectric-insulator-semiconductor (MFIS) structures have been studied extensively [11-16]. However, satisfactory understanding in all details has still not been achieved. At high frequencies ω the charges at the interface states cannot follow an ac signal. In contrary, at low frequencies the charges can easily follow an ac signal and they are capable of these charges increase with decreasing frequency. Therefore, the frequency and temperature dependent dielectric properties are very important for accurate and reliable results [17-22].

In our previous study [23], we studied experimentally the frequency dependence of *C-V* and *G/ω-V* characteristics of MFIS structures by considering the N_{ss} and R_s effects. We found both the *C-V* and *G/ω-V* characteristics are strongly frequency and voltage dependent and exhibit anomalous peaks at forward bias due to the N_{ss} and R_s. Therefore, in this work, our aim is to investigate experimentally the frequency and temperature dependence of forward and reverse dielectric properties of $Au/Bi_4Ti_3O_{12}/SiO_2/Si$ (MFIS) structures under forward and reverse bias were studied in the frequency and temperature range of range of 1 kHz-5 MHz and 80-400 K, respectively. Experimental results show that the dielectric constant (ε'), dielectric loss (ε''), dielectric loss tangent (tanδ) and the ac electrical conductivity (σ_{ac}) strongly frequency and temperature dependent.

2. Experimental procedure

In this study, the $Bi_4Ti_3O_{12}$ (BTO) thin films were deposited on Si substrate with magnetron sputtering by using a hot compacting of $Bi_4Ti_3O_{12}$ powder of a stochiometric composition as a target material. The mixture of Ar and O_2 was used a working medium and the

substrate was kept at 700 ^oC. The thicknesses of the deposited BTO thin films were measured by Veeco Dektak 6M thickness profilometer and found to be around 2.4 μm. The chemical composition of films was determined by local X-ray spectral method on scanning electron microscope REM-101M by comparing the spectral line intensity of the films with standard sample. The thin layer of silicon dioxide (SiO_2) at the BTO/Si interface was assumed to be formed during annealing of the BTO films in air ambient [8]. For electrical measurements, the pure Au (99.999 %) circular dots with the thickness of about 2000 Å in a diameter of 1 mm were deposited by e-beam evaporator through a shadow mask on the BTO films as top contact and bottom contact were also produced by the same way on the back of the Si substrate as to form a MFIS structure. The ohmic contacts were prepared by sintering the evaporated back contact at about 700 ^oC for 20 minute in flowing dry nitrogen (N_2) ambient at rate of 1.5 l/min. This process served to sinter the Au on upper surface of the n-type Si wafer. In this way, $Au/Bi_4Ti_3O_{12}/SiO_2/n$-Si (MFIS) structures were fabricated on the n-type Si wafer. The electrode connections were made by silver paste. Impedance measurements (C-V and G/ω-V) were carried out using a Hewlett-Packard HP 4192A LF impedance analyzer (5 Hz-13 MHz) which was controlled by a microcomputer. The impedance characteristics were measured by applying a small ac signal of 40 mV amplitude in 1kHz-5 MHz frequency range while the gate bias was sequentially swept from negative bias (-6 V) to positive bias (6 V).

3. Results and discussion

3.1. Frequency dependence of dielectric properties and electrical conductivity

The frequency dependence of the real part of complex permittivity ε' (dielectric permittivity), and the imaginary part of complex permittivity ε'' (dielectric loss factor), loss tangent (tanδ), ac electrical conductivity (σ_{ac}) and the complex electric modulus (M' and M'') were studied for $Au/Bi_4Ti_3O_{12}/SiO_2/Si$ (MFIS) structures. The values of the dielectric properties were calculated as a function of frequency in the frequency range of 1 kHz-5 MHz and at the temperature range of 80 K- 400 K, respectively. The complex permittivity can be defined in the following complex form [24,25]

$$\varepsilon^* = \varepsilon^{'} - j\varepsilon^{''} \tag{1}$$

where j is the imaginary root of -1. The complex permittivity formula has been employed to describe the electrical and dielectric properties. In the ε* formulation, in case of admittance measurements (C-V and G/ω-V), the following relation holds:

$$\varepsilon^* = \frac{Y^*}{j\omega C_o} = \frac{C}{C_o} - j\frac{G}{\omega C_o} \tag{2}$$

where Y^*, C and G are the measured admittance, capacitance and conductance of the dielectric, respectively, and ω is the angular frequency (ω=2πf) of the applied electric field [26]. The dielectric constant (ε'), at various frequencies was calculated by using the measured capacitance values at the strong accumulation region via the formula [27,28]:

$$\varepsilon^{'} = \frac{C}{C_o} \tag{3}$$

where C_o is capacitance of an empty capacitor. $C_o = \varepsilon_o(A/d)$; where A is the rectifier contact area in cm^{-2}, d is the interfacial insulator layer thickness and ε_o is the permittivity of free space charge (ε_o = $8.85x10^{-14}$ F/cm). In strong accumulation region, the maximal capacitance of devices corresponds to the insulator layer capacitance ($C_{ac} = C_{ox} = \varepsilon^{'}\varepsilon_o A/d$). The dielectric loss (ε''), at various frequencies was calculated by using the measured conductance values from the relation,

$$\varepsilon^{''} = \frac{G}{\omega C_o} \tag{4}$$

The loss tangent (tanδ) can be expressed as follows [24,25,29-31],

$$\tan\delta = \frac{\varepsilon^{''}}{\varepsilon^{'}} \tag{5}$$

The effect of conductivity can be highly suppressed when the data are presented in the modulus representation. The dielectric modulus *(M*)* corresponds to the relaxation of the electric field in the material when the electric displacement remains constant. The starting point for further consideration is the definition of the dielectric modulus:

$$M^*(\omega) = 1/\varepsilon^*(\omega) = M'(\omega) + jM''(\omega) \tag{6a}$$

The complex electric modulus is derived from the complex permittivity, according to the relationship defined by Macedo et al. [32]. The real *(M')* and imaginary *(M'')* parts of the complex electrical modulus were obtained from *ε'(ω)* and *ε''(ω)* values, as follows [33]:

$$M'(\omega) = \frac{\varepsilon'(\omega)}{\varepsilon'(\omega)^2 + \varepsilon''(\omega)^2}$$

and

$$M''(\omega) = \frac{\varepsilon''(\omega)}{\varepsilon'(\omega)^2 + \varepsilon''(\omega)^2} \tag{6b}$$

Based on these equations, we have changed the form of presentation of the dielectric data from *ε'(ω)* and *ε''(ω)* to *M'(ω)* and *M''(ω)*. The ac electrical conductivity (σ_{ac}) of the dielectric materials is proportional to tanδ, namely ε'' can be given by the following equation [24,34,35],

$$\sigma_{ac} = \omega C \tan\delta (d / A) = \varepsilon^{"} \omega \varepsilon_o \qquad (7)$$

where, ε_0 is the dielectric constant of free space and ω is the angular frequency.

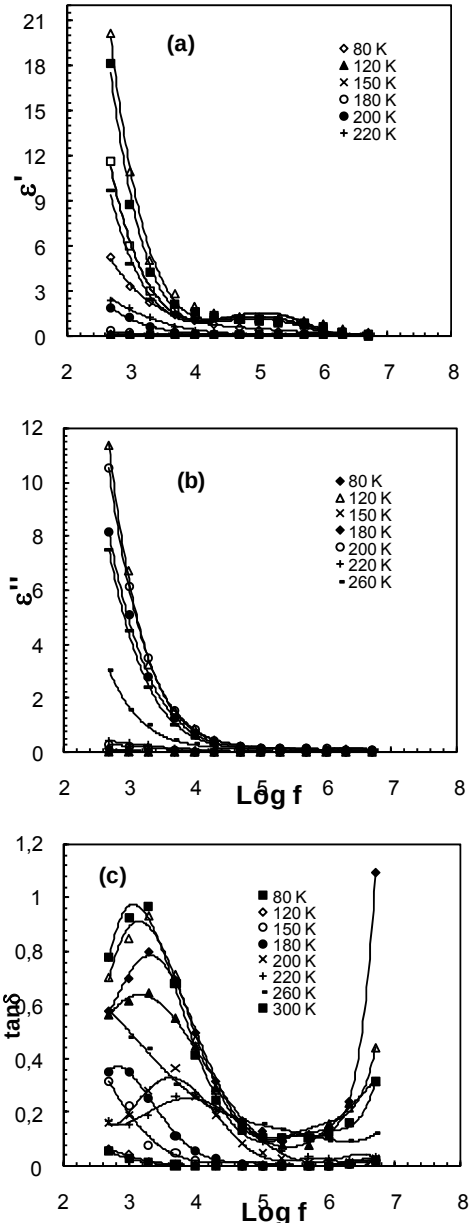

Fig.1. The frequency dependence of the (a) ε', (b) ε'' and (c) tanδ for $Au/Bi_4Ti_3O_{12}/SiO_2/Si$ (MFIS) structure at various temperatures.

The impedance measurements for a dc bias at accumulation region can provide us with the dielectric constant and dielectric loss as a function of frequency. The frequency response of the ε', ε'' and tanδ of $Au/Bi_4Ti_3O_{12}/SiO_2/Si$ (MFIS) structure at various temperature are depicted in Fig. 1(a), (b) and (c), respectively. From the measured values of capacitance and conductance at strong accumulation region, the values of the ε', ε'' and tanδ were found to be strongly dependent to frequency and temperature. However, this change is very small at low temperatures. In principle, at low frequencies and temperature, all the four types of polarization processes, i.e., the electronic, ionic, dipolar, and interfacial or surface polarization contribute to the values of ε' and ε''. It is noticed that both ε' and ε'' increase with decreasing frequency at all temperatures. Also, especially at high frequency, the value of ε' becomes closer to the values of ε'' due to interface states (N_{ss}) that can not follow the ac signal at enough high frequency ($f \geq 500$ kHz). This behavior is more pronounced below 10 kHz frequencies. The increase in ε' and ε'' with decrease in frequency reveals that there are strong interfacial polarization especially at low frequency. Because the interfacial polarization can be more easily occur at the lower frequency and with the number of surface states between the insulator layer and semiconductor, consequently, this contributes to the improvement of the dielectric properties of the MFIS structure. The variation of the loss tangent (tanδ) with respect to frequency of $Au/Bi_4Ti_3O_{12}/SiO_2/Si$ (MFIS) structure is shown in Fig. 1(c). As shown in figure, the loss tanδ decreases with increasing frequency at low frequencies and temperatures. It is clear that tan δ is in close relation with the conductivity.

Fig. 2 illustrates the dependence of the ac electrical conductivity (σ_{ac}) on the frequency at various temperatures (in the frequency range 1 kHz-5 MHz and 80 K- 400 K temperature) for $Au/Bi_4Ti_3O_{12}/SiO_2/Si$ (MFIS) structure. As can be seen from Fig. 2 at low frequencies the value of σ_{ac} tends to be constant, while at higher frequencies it becomes frequency dependent as a power of frequency. Also, it is noticed that the ac electrical conductivity generally increase with increasing frequency and temperature and especially there is a sharp increase in the σ_{ac} after about 100 kHz. Similar behavior was observed in the literature [36-39].

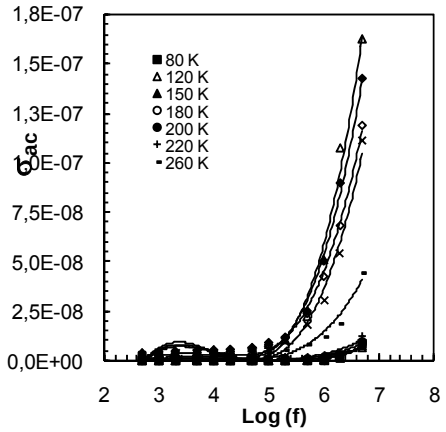

Fig. 2. The frequency response of the σ_{ac} for $Au/Bi_4Ti_3O_{12}/SiO_2/Si$ (MFIS) structure at various temperatures.

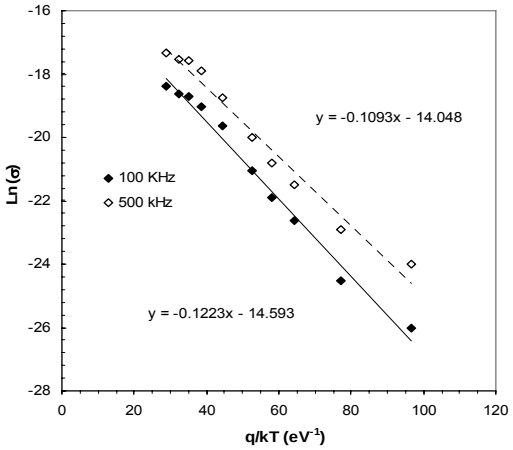

Fig. 3. Electrical conductivity (σ_{ac}) vs q/kT of $Au/Bi_4Ti_3O_{12}/SiO_2/Si$ (MFIS) structure at 100 kHz and 500 kHz.

The electrical conductivity of MIS or MFIS depends upon numerous factors. The nature of dopant material, the process of doping, and the formation of interfacial insulator layer and interface states localized between semiconductor and insulator layer have been found to play a vital role in controlling the conductivity. There have been several reports [36-42] in which the temperature dependent conductivity data of MIS or MFIS structures have been fitted to the Arrhenius equation of conductivity. The temperature dependence of electrical conductivity (σ_{ac}) is shown in Fig.3. As can be seen in Fig. 3, there is a linear relationship between the total conductivity and the inverse temperature could be written as [22],

$$\sigma(T) = \sigma_0 \exp\left(-\frac{E_a}{kT}\right) \tag{7}$$

where E_a is the activation energy, k is the Boltzman constant, T is the absolute temperature and σ_0 is the electrical conductivity as $T\rightarrow\infty$. The activation energy (E_a) of the conduction mechanism was computed by using the Arrhenius plot for 100 kHz and 500 kHz, and values of 122.3 meV and 109.3 meV, respectively, were obtained. These values are far away from the mid-gap energy, which is around 2 eV for $Bi_4Ti_3O_{12}$. Thus, it can be assumed that the observed exponential behavior is not due to intrinsic conduction. From the same Arrhenius plot, the parameter σ_o can be calculated as $4.6\text{x}10^{-7}$ $(\Omega.\text{cm})^{-1}$ and $7.93\text{x}10^{-7}$ $(\Omega.\text{cm})^{-1}$ for 100 kHz and 500 kHz, respectively. As expected, the electrical conductivity (σ_{ac}) depends on frequency and temperature.

3.2. Temperature dependence of dielectric properties and electrical conductivity

The temperature response of the ε', ε'' and tanδ of $Au/Bi_4Ti_3O_{12}/SiO_2/Si$ (MFIS) structure at two different frequencies calculated from Eqs. (3), (4) and (5) and are given in Fig. 4(a), (b) and (c), respectively. From the measured values of capacitance and conductance at strong accumulation region, the values of the ε', ε'' and tanδ were found to strongly depend on temperature. However, this change is very small at low temperatures. Fig. 4 (a), (b) and (c) indicate that the values of ε', ε'' and tanδ increase with increasing temperature and they give a maxima which shifted towards the higher temperatures as the measuring frequency is increased.

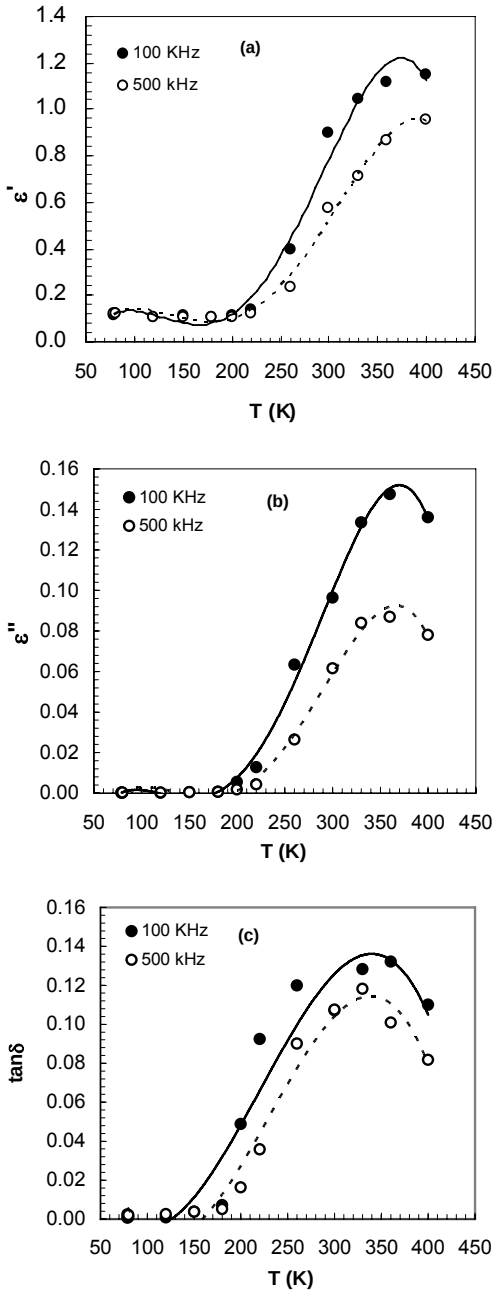

Fig.4. The temperature dependence of the (a) ε', (b) ε'' and (c) tanδ for $Au/Bi_4Ti_3O_{12}/SiO_2/Si$ (MFIS) structure, respectively, at 100 kHz and 500 kHz.

The electric modulus representations of dielectric process provide a good qualitative description of the dielectric relaxation. Therefore, many authors prefer to describe the dielectric properties of MIS or MFIS structures by using the dielectric modulus [36,40-42]. The real *(M')* and imaginary *(M")* component of the electrical modulus were calculated from the values of ε' and ε'' for two different frequencies by using Eq. 6, and are given in Fig 5(a) and (b) respectively. The value of real component M' decreases with increasing temperature up to room temperature, and then becomes independent of temperature and frequency. In other words, M' reaches a maximum constant value depending to $M_\infty=1/\varepsilon_\infty$ to relaxation process. On the other hand, a peak is observed in the imaginer component M", which shifts to higher temperature with increasing frequency.

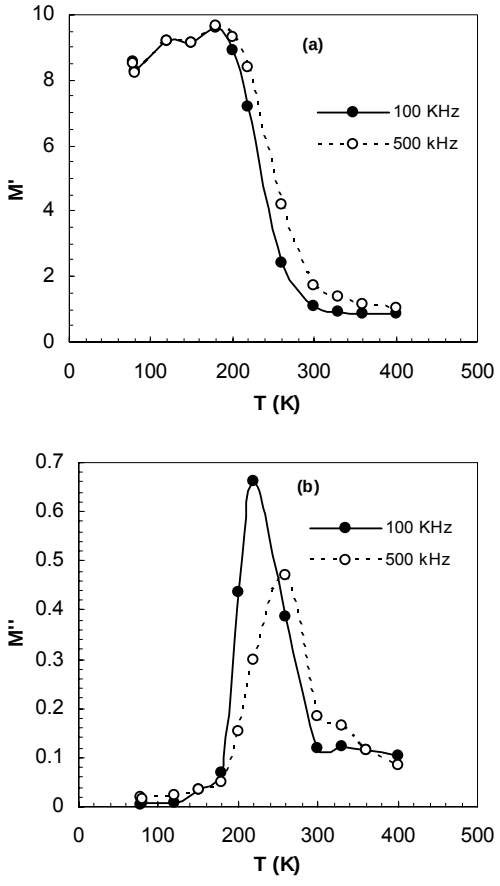

Fig. 5. Real and imaginary part of electric modulus M' (a) and M" (b) vs temperature.

4. Conclusions

Frequency and temperature dependence of electrical and dielectric properties of $Au/Bi_4Ti_3O_{12}/SiO_2/Si$ (MFIS) structure have been studied in detail in the wide temperature (80-300 K) and frequency (1 kHz-5 MHz) range by using C-V and G/ω-V measurements. The values of real part of dielectric permittivity (ε'), dielectric loss (ε"), loss tangent (tanδ) and ac electrical conductivity (σ_{ac}) of $Au/Bi_4Ti_3O_{12}/SiO_2/Si$ (MFIS) structure, strongly depends on frequency and temperature. The values of ε' and ε" decrease with increasing frequency while increase with increasing temperature. At low frequencies the value of σ_{ac} tends to be constant, while at higher frequencies it becomes frequency dependent as a power of frequency. The interfacial polarization can be more easily occurred at low frequencies, because at low frequencies the charges at interface can easily follow an ac signal and they are capable of increase these charges with decreasing frequency. The value of real component M' decreases with increasing temperature up to room temperature, and then becomes independent of temperature and frequency. On the other hand, a peak is observed in the imaginer component M", which shifts to higher temperature with increasing frequency. It is concluded that the values of ε', ε'', tan δ, M' and M'' in MFIS structure are strongly dependent on both the frequency and temperature.

References

[1] J. L. Moll, Y. Tarui: IEEE Trans. Electtron Devices **10**, 338 (1963).
[2] K. Sugibuchi, Y. Kurogi, N. Endo: J. Appl. Phys. **46**, 2877 (1975).
[3] S. Y. Wu, W. J. Takei, M. H. Francombe, Ferroelectrics **10**, 209 (1976).
[4] W.P. Li, Y.M. Liu, R.Zhang, J. Chen, P. Cheng, X. L. Yuan, Y. G. Zhou, B. Shen, R. L. Jiang, Y. Shi, Z. G. Liu, Y. D. Zheng, Appl. Phys. A **72**, 85 (2001).
[5] J.F. Scott, Ferroelectr. Rev. **1**, 1 (1991).
[6] K. Aizawa, E. Tokumitsu, K. Okamoto, H. Ishawara, Appl. Phys. Lett. 7 (2000) 2609.
[7] B. H. Park, B. S. Kang, S. D. Bu, T. W. Noh, J. Lee, W. Jo, Nature (London) **401**, 682 (1999).
[8] P. C. Joshi, S. B. Krupanidhi: J. Appl. Phys. **72**, 5827 (1992).
[9] K. J. Choi, W. C. Shin, J. H. Yang, S. G. Yoon, Appl. Phys. Lett. **75**, 722 (1999).
[10] C. H. Huang, T. Y. Tseng, C. H. Chien, M. J. Yang, C. C. Leu, T. C. Chang, P. T. Liu, T. Y. Huang, Thin Solid Films, **420**, 377 (2002).
[11] C. Huang, Y. Wang, H. Lue, J. Huang, M. Lee, T. Tseng, Journal of European Ceramic Society, **24**, 2471 (2004).
[12] K. Kim, C. Kim, Thin Solid Films **478**, 6 (2005).
[13] T. Shao, T.Ren, C. Wei, X. Wang, C. Li, J. Liu, L. Liu, J. Zhu, Z. Li, Integrated Ferroelectrics **57**, 1241 (2003).
[14] M. Ryu, S. H. Lee, J. H. Ro, J. P. Kim, H. J. Joo, M. S. Jang, Ferrolectrics, **271**, 211 (2002).
[15] N. Kumari, J. Parii, K. B. R. Varma, S. B. Krupandhi, Solid State Communications **137**, 566 (2006).
[16] F. M. Pontes, E. R. Leite , E J. H. Lee , E. Longo, J.A. Varela, Thin Solid Films **385**, 260 (2001).
[17] H. Deuling, E. Klausmann, A. Goetzberger, Solid State Electron. **15**, 559 (1972).

[18] M. Depas, R. L. Van Meirhaeghe, W. H. Lafere, F. Cardon, Solid State Electron. **37**, 433 (1994).
[19] R. Castagne, A. Vapaille, Surface Science **28**, 157 (1971).
[20] U. Kelberlau, R. Kassing, Solid State Electron. **22**, 37 (1979).
[21] M. Kuhn, Solid State Electron. **13**, 873 (1970).
[22] S. Kar, S. Varma, J. Appl. Phys. **58**, 4256 (1985).
[23] F. Parlaktürk, Ş. Altındal, A. Tataroğlu, M. Parlak, A. Agasiev, Microelect. Eng. **85**, 81 (2008).
[24] C. P. Symth, Dielectric Behaviour and Structure, McGraw-Hill, New York, 1955.
[25] Vera V. Daniel, Dielectric Relaxation, Academic Press, London, 1967.
[26] P. Pissis, A. Kyritsis, Solid State Ionics **97**, 105 (1997).
[27] A. Chelkowski, Dielectric Physics, Elsevier, Amsterdam, 1980.
[28] A. Tataroğlu, Microelectron. Eng. **83**, 2551 (2006).
[29] M. Popescu, I. Bunget, Physics of Solid Dielectrics, Elsevier, Amsterdam, 1984.
[30] A. Chelkowski, Dielectric Physics, Elsevier, Amsterdam, 1980.
[31] A. Tataroğlu, Ş. Altındal , M.M. Bülbül, Microelect. Eng. **81**, 140 (2005).
[32] P. B. Macedo, C. T. Moynihan, R. Bose, Phys Chem Glasses **13**, 171 (1972).
[33] M. K. Ram, S. Annapoorni, S. S. Pandey, B. D. Malhotra, Polymer **39**, 3399 (1998).
[34] M. S. Mattsson, G. A Niklasson, K. Forsgren, A. Harsta, J. Appl. Phys. **85**, 2185 (1999).
[35] K. Prabakar, S. K. Narayandass, D. Mangalaraj, Phys. Stat. Sol. (a) **199**, 507 (2003).
[36] M. D. Migahed, M. Ishra, T. Fahmy, A. Barakat, J. Phys. and Chem. Solids, **65**, 1121 (2004).
[37] S. P. Szu, C. Y. Lin, Mater. Chem. and Phys. **82**, 295 (2003).
[38] D. Maurya, J. Kumar, Shripal, J. Phys. and Chem. Solids **66,** 1614 (2005).
[39] A. A. Sattar, S. A. Rahman, Phys. Stat. Sol. (a) **200**, 415 (2003).
[40] C. Fanggao, G. A. Saunders, E. F. Lambson, R. N. Hampton, G. Carini, G. D. Marco, M. Lanza, J. Appl. Poly. Sci. **34**, 425 (1996).
[41] S.A. Nouh, S.A. Gaafar, H.M. Eissa, Phys. Stat. Sol. (a) **175**, 699 (1999).
[42] M. R. Ranga Raju, R. N. P. Choudhary, S. Ram, Phys. Stat. Sol. (b) **239,** 480 (2003).

*Corresponding author: ademt@gazi.edu.tr